Journal of Materials Chemistry C

ROYAL SOCIETY OF CHEMISTRY

PAPER

View Article Online
View Journal | View Issue

Check for updates

Cite this: J. Mater. Chem. C, 2023, 11, 8100

Shape programming and photoactuation of interpenetrating polymer networks containing azobenzene moieties†

Toru Ube, *[a] Keigo Naito[b] and Tomiki Ikeda *[a]

Received 26th September 2022,
Accepted 29th November 2022

DOI: 10.1039/d2tc04067k

rsc.li/materials-c

Crosslinked liquid-crystalline polymers (LCPs) with photochromic moieties exhibit macroscopic deformation upon irradiation with light. Controlling the 3D shapes of crosslinked LCPs leads to fabrication of photoactuators with desired structures and functions. Here, we investigate the shape memory effects and photoinduced deformation of interpenetrating polymer network (IPN) films composed of azobenzene LCP (PAzo) and poly(methyl methacrylate) (PMMA). PAzo/PMMA IPN films could be temporarily programmed into desired 3D structures with the aid of glass transition. The IPN films with temporary shapes showed high thermal stability compared to pristine PAzo films, which is ascribed to the gradual glass transition behaviour over a wide temperature range. The shape-programmed IPN samples showed various reversible deformation behaviours depending on the programmed shapes upon irradiation with UV and visible light. Furthermore, the thermal stability of temporary shapes allowed reversible photoactuation of shape-programmed samples at elevated temperatures as high as 100 °C. Formation of IPN films is a promising approach to enhance the design and functions of photoactuators consisting of crosslinked LCPs.

Published on 09 1401. Downloaded on 25/02/1405 11:07:51 ..

10th Anniversary Statement

Tomiki Ikeda served as an Associate Editor of *J. Mater. Chem.* during 2007–2010 and on the International Advisory Editorial Board during 2010–2013. At that time, the Materials Editorial Board (MEB) was very keen to attract researchers in the materials chemistry field through short publication times and high impact factors, and through the following strong promotions, the number of submissions increased drastically. As a result, each printed version became thicker and thicker. It was a wise decision that the journal was divided into 3 parts, A, B, & C. Currently, there are so many journals in the materials chemistry field, but I'm sure that *J. Mater. Chem.* will continue to play a major and leading role in this field as before.

Introduction

Liquid-crystalline polymers (LCPs) have been extensively studied as functional materials with stimuli responsive properties due to the strong coupling between the alignment of mesogens and conformation of polymer chains.[1–3] LCPs with chemically crosslinked structures show macroscopic deformation under stimuli, such as heat, electricity and light, along with the change in alignment of mesogens. Crosslinked LCPs with photochromic moieties, represented by azobenzene derivatives, exhibit reversible deformation upon irradiation with light.[3–8] Crosslinked azobenzene LCP films with in-plane uniaxial alignment typically bend upon irradiation with UV light as a result of contraction of the surface region of the sample and revert to the initial shape upon irradiation with visible light. This reversibility of deformation is ensured by the shape memory effects of crosslinked networks. Conventional preparation procedures of crosslinked LCPs with uniaxial alignment, such as two-step crosslinking[9] and *in situ* polymerization in cells,[10] yield flat films. The flat shapes are permanently memorized by chemical networks during crosslinking processes.

Photoinduced deformation of LCPs strongly depends on the initial shapes, initial alignment of mesogens, and irradiation conditions (*i.e.*, spatial and temporal distribution of light intensity). By controlling these parameters, various photoinduced motions, such as bending,[4] rotation,[11] locomotion,[12–14] oscillation,[15–17] and liquid transport,[18] have been demonstrated.[3–8] The initial alignment of mesogens has been controlled using external force, electromagnetism, and the surface alignment technique. Recent

[a] Research & Development Initiative, Chuo University, 1-13-27 Kasuga, Bunkyo-ku, Tokyo 112-8551, Japan. E-mail: ube@tamacc.chuo-u.ac.jp tikeda@tamacc.chuo-u.ac.jp
[b] Graduate School of Science and Engineering, Chuo University, 1-13-27 Kasuga, Bunkyo-ku, Tokyo 112-8551, Japan

† Electronic supplementary information (ESI) available: Fig. S1–S3 (PDF) and Movies S1–S5 (MP4). See DOI: https://doi.org/10.1039/d2tc04067k

This journal is © The Royal Society of Chemistry 2023

Published on 09 1401. Downloaded on 25/02/1405 11:07:51 ..

development of the photoalignment technique has enabled patterning of LCPs, which leads to complicated deformation due to the spatial distribution of photoinduced strain.[19–22] As the alignment of mesogens is coupled with the conformation of polymer chains in LCPs, their initial shapes can also be controlled simultaneously with the alignment of mesogens through these processes. In crosslinked LCP films with spatially varying director patterns, the films crosslinked at elevated temperatures in flat cells often show non-flat 3D shapes at room temperature. This spontaneous deformation originates from the inhomogeneity of strain that develops during the cooling process from the crosslinking temperature due to the temperature dependence of the LC order.[23,24] Moreover, an increase in the variety of macroscopic architectures has been achieved by applying 3D printing technology to the fabrication processes of crosslinked LCPs.[25,26] As clarified in these examples, 3D structures can be programmed in the samples during the formation of crosslinked structures.

In addition, the control of initial shapes after the formation of crosslinked structures has also been studied, expanding the diversity of photoinduced motions with reconfigurable structures. Rearrangement of network structures has been realized by introducing dynamic covalent bonds.[27–33] Exchange reactions, such as transesterification, have been applied to LCPs, enabling the alteration of initial shapes. Shape programming has also been demonstrated in crosslinked LCPs with permanent networks by the combination of photochemical and photothermal processes.[34] Photochemical deformation with patterned irradiation defines initial shapes for the subsequent reversible photothermal actuation. Furthermore, patterning of the photoactuation area has been achieved by acid treatment for pH-sensitive photochromic dyes.[35]

Various shapes of polymer materials in general can be achieved with the aid of glass transition. A temporary shape, which is formed with an external force above the glass transition temperature (T_g), can be fixed by cooling below T_g. In crosslinked polymers, the initial permanent shape is recovered by reheating above T_g. This process of shape programming and recovery has also been applied to induce one-time deformation of polymer materials from temporary to permanent shapes under stimuli, such as heat and light.[36–38] Shape programming with the aid of glass transition would be applicable to crosslinked LCPs with sufficiently high T_g to achieve reversible photoactuation of 3D temporary shapes. However, photoresponsive crosslinked LCPs with glassy nature typically show a low T_g of 20–60 °C: Glassy crosslinked LCPs with a T_g slightly higher than room temperature often show fast deformation due to the high efficiency of the change in the alignment of mesogens and conformation of polymer chains. In these systems, shape memory with glass transition is not satisfactory in obtaining photomobile materials with sufficient thermal stability of temporary shapes. Verpaalen *et al.* recently reported an approach for shape memory of photomobile polymer materials by preparation of a bilayer structure of crosslinked LCPs and poly(ethylene terephthalate) (PET) through the spray-coating process.[39] The bilayer films showed shape programmability under heating with the aid of the thermoplastic properties of PET substrates. PET also acts as an alignment layer for the splay-coated LCs. As shown in this example, the combination of multiple components is an effective approach to allow shape programming of crosslinked LCPs. We previously developed photomobile materials with interpenetrating polymer network (IPN) structures composed of crosslinked LCPs and photoinert amorphous polymers and reported control of their mechanical and photoresponsive properties through the selection of amorphous components.[40,41] In particular, incorporation of soft polymers, such as poly(dodecyl methacrylate) and poly(dimethyl siloxane), resulted in the enhancement of photoinduced bending properties of flat films due to the decrease in elastic modulus. IPNs containing LCPs have also been applied to photonic materials,[42] tough LC elastomers,[43,44] and shape memory materials.[45,46] The strategy of introducing additional components into crosslinked LCPs by the formation of IPN structures would be feasible to control the T_g and shape memory behaviour of photomobile materials.

The shape memory effects of IPNs (or semi-IPNs) have previously been studied for those with photoinert components,[45–50] such as poly(methyl methacrylate) (PMMA) and poly(ethylene glycol) (PEO),[47,48] and LCPs with phenyl benzoate mesogens.[45,46] These IPNs typically show multiple transition temperatures and/or gradual glass transition over a broad temperature range, which contribute to shape memory effects. In this study, we investigate the shape memory effects of IPN films composed of crosslinked azobenzene LCP (PAzo) and PMMA (Scheme 1a) and compared them with those of pristine PAzo films. Photoinduced deformation was demonstrated for IPN films after shape programming.

Experimental

Materials and methods

Scheme 1b shows the chemical structures of the compounds used in this study. A6AB6 and DA6AB were synthesized according to the previously reported procedures.[51] 1BZ6 was synthesized through the esterification of *p*-anisic acid and 4-hexyloxyphenol in dichloromethane catalysed by *N*,*N*′-dicyclohexylcarbodiimide (DCC) and 4-dimethylaminopyridine (DMAP). Differential scanning calorimetry (DSC) was performed on a DSC-60 (Shimadzu). FTIR spectra were recorded using a spectrometer (JASCO, FT/IR-4200). Polarized absorption spectra were recorded with a spectrometer (JASCO, V-630) using a Glan–Thompson prism. The mechanical properties of polymer films were evaluated using a digital force gauge (Imada, ZTA5N) and a motorized test stand (Imada, MX2-500N) at a constant elongation speed of 10 mm min^{-1}. Young's modulus, E, was evaluated as a ratio of stress to strain in a small strain limit. Photoinduced deformation of polymer films was observed using a CCD camera (Artray, ARTCAM-130SN) equipped with CCTV lens (EMVL-MP3020, Misumi) upon irradiation with UV light (365 nm) from UV-LED (NS lighting, ULEDN-102CT), and visible light ($>$540 nm) from a halogen lamp (Tokina, KTX-100E) through glass filters (Tokina, Y52 and HA50). Real-time absorption spectra under irradiation with UV light were recorded with a multichannel spectrometer

Published on 09 1401. Downloaded on 25/02/1405 11:07:51 ..

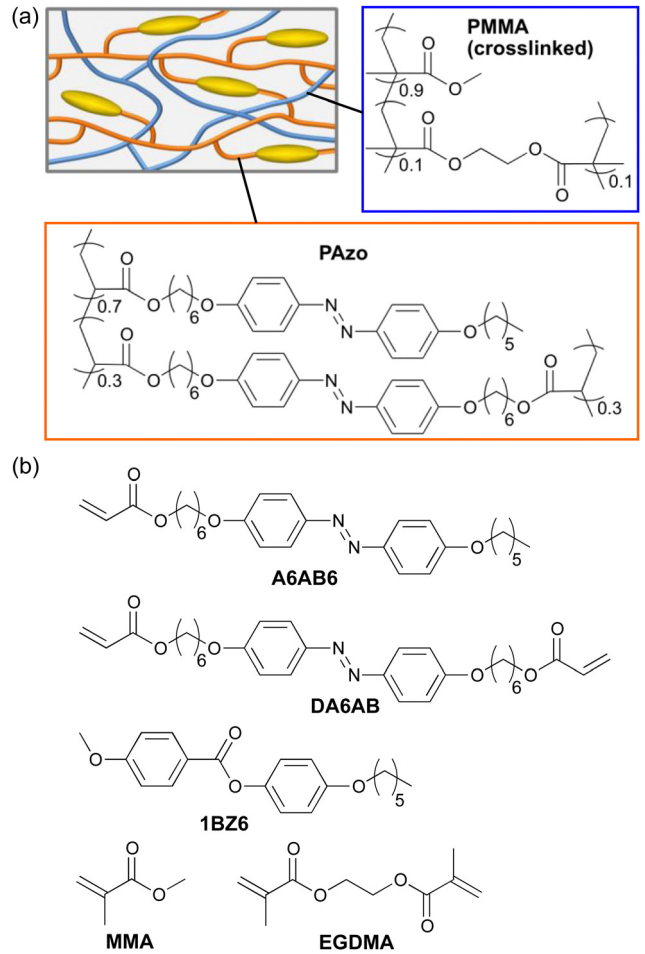

Scheme 1 (a) Schematic illustration of the IPN. (b) Chemical structures of compounds used in this study.

(Ocean optics, Flame-S-XR1-ES) using a halogen lamp (Philips, 7027) as a probe light source.

Preparation of PAzo/PMMA IPN films

A mixture of A6AB6 (35 mol%), DA6AB (15 mol%), a photoinitiator (Irgacure 784, 2 mol% of the monomers) and 1BZ6 (50 mol%) was injected into a glass cell coated with in-plane uniaxial or homeotropic alignment layers at 90 °C (isotropic phase): the glasses had been coated with rubbed polyimide for in-plane uniaxial alignment, while those had been treated with octadecyltrimethoxysilane for homeotropic alignment. After the mixture was cooled down (0.5 °C min^{-1}) to the LC temperature (72 °C), photopolymerization was carried out with light (>540 nm, 2 mW cm^{-2}) from a 500 W super high pressure mercury lamp through glass filters (Tokina, Y52 + HA50) for 2 h. After the formation of the PAzo network, the cells were immersed in acetone to remove 1BZ6. Then, the cells were immersed in a mixture of MMA (90 mol%), EGDMA (10 mol%) and 2,2′-azobisisobutyronitrile (1 mol% of the monomers). Thermal polymerization was performed at 65 °C for 3 h on a hot plate under an argon atmosphere. The film was removed from the cell and washed with methanol.

Preparation of pristine PAzo films

A mixture of A6AB6 (70 mol%), DA6AB (30 mol%), and a photoinitiator (Irgacure 784, 2 mol% of the monomers) was injected into a glass cell coated with in-plane uniaxial or homeotropic alignment layers at 110 °C (isotropic phase). After the mixture was cooled down (0.5 °C min^{-1}) to LC temperature (88 °C), photopolymerization (>540 nm, 2 mW cm^{-2}) was carried out for 2 h. The film was removed from the cell and washed with methanol.

Results and discussion

Shape memory effects

IPN films were prepared by sequential formation of PAzo and PMMA networks. Formation of PMMA in the PAzo network was confirmed with FTIR spectra: absorption was significantly increased significantly at 2992, 1450, 990 and 750 cm^{-1} (methyl and methylene), as well as at 1730, 1250 and 1150 cm^{-1} (ester). The weight ratio of PAzo and PMMA networks in IPN films was evaluated from the weights of films before and after the formation of PMMA networks: PAzo/PMMA = 55/45.

Fig. 1a shows the DSC thermograms of pristine PAzo and PAzo/PMMA IPN samples. The DSC thermogram of pristine PAzo shows a baseline shift at 45–70 °C, which corresponds to T_g. For PAzo/PMMA, on the other hand, T_g was not clearly observed in the DSC thermogram. This behaviour would be indicative of the gradual glass transition over a wide temperature range. LC–isotropic transition was not observed for both samples, which is characteristic in highly crosslinked LC networks.[52]

To further elucidate the glass transition behaviour, the temperature dependence of elastic modulus was examined for the films with in-plane uniaxial alignment (Fig. 1b). On heating from room temperature, the pristine PAzo film showed a rapid decrease in E at temperatures below 70 °C and exhibited plateau above 70 °C, which is consistent with the DSC result. PAzo/PMMA, on the other hand, showed a gradual decrease in E over a wide temperature range up to 180 °C: from $E \approx 1$ GPa at 30 °C to $E \approx 40$ MPa at 180 °C, which indicate the transition from glassy to rubbery states. Gradual transition is one of the typical properties of IPN systems, originating from complicatedly mixed structures of multiple components,[53,54] which has also been reported for IPNs containing LCPs.[45,46,55] From a molecular viewpoint, the fraction of polymer chain segments capable of micro-Brownian motions gradually increases with temperature in IPNs.

We next examined the shape memory effects of pristine PAzo and PAzo/PMMA IPN films with in-plane uniaxial alignment of mesogens (Fig. 1c–f). As the films were obtained by polymerization and crosslinking in glass cells, flat shapes were memorized as permanent shapes. The initial flat shapes were transformed into curved shapes by fixing around a rod under heating at 100 °C and cooling to room temperature. Both films could memorize curved states as temporary shapes, and the IPN film showed larger curvature than the pristine PAzo film. When the curved samples were subjected to reheating, the curved PAzo

 This journal is © The Royal Society of Chemistry 2023

Published on 09 1401. Downloaded on 25/02/1405 11:07:51 ..

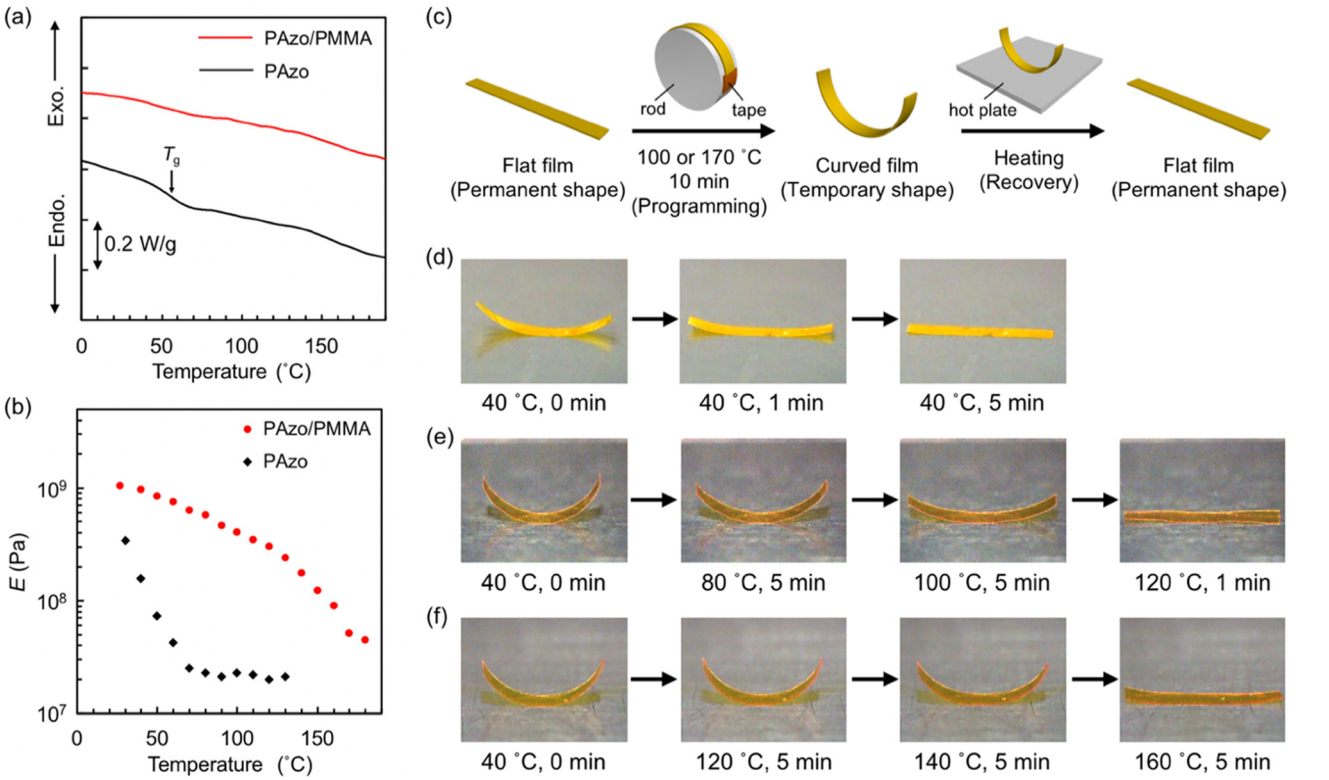

Fig. 1 (a and b) Thermal and mechanical properties of PAzo/PMMA IPN and pristine PAzo. (a) DSC thermograms at a heating rate of 20 °C min^{-1}. (b) Temperature dependence of elastic moduli for uniaxially aligned films, which were obtained by uniaxial extension in the alignment direction of mesogens. (c) Schematic illustration of shape memory tests. (d–f) Shape recovery for films of (d) PAzo programmed at 100 °C, (e) PAzo/PMMA IPN programmed at 100 °C, and (f) PAzo/PMMA IPN programmed at 170 °C. Sizes of the films: 8 mm × 1 mm × 20 μm.

film reverted to a flat state (permanent shape) at 40 °C (Fig. 1d). On the other hand, the shape recovery of PAzo/PMMA was small at 40 °C (Fig. 1e). The curved shape was preserved at 80 °C, although the curvature was decreased. Further heating at 100 °C resulted in an almost flat shape. The curved IPN film programmed at 170 °C showed enhanced thermal shape stability: The curved shape was preserved at 120 °C and reverted to the flat shape at 160 °C (Fig. 1f). On shape programming at higher temperatures, the larger fraction of polymer chain segments would adapt to force and contribute to the stabilization of temporary shapes through micro-Brownian motions. For the recovery of a permanent flat shape, a sufficiently high temperature is needed to allow relaxation of the chain segments that support a temporary shape. This relationship between programming and recovery temperatures was similar to those reported for other materials with broad glass transition, such as nanocomposites[56] and Nafion.[57] The enhanced stability of temporary shapes in crosslinked LCPs by the formation of IPN structures would lead to reversible photoactuation of non-flat samples with various initial shapes.

Photoinduced deformation behaviour

Photoinduced bending behaviour was investigated for PAzo/PMMA IPN films. The alignment of azobenzene moieties in in-plane uniaxial and homeotropic films was confirmed by polarized absorption spectroscopy (Fig. S2, ESI†). As shown in Fig. 2a, a flat film with the in-plane uniaxial alignment of mesogens bends toward the light source upon irradiation with UV light. Then, it reverted to the initial flat shape upon irradiation with visible light. This bending behaviour is similar to those of crosslinked LCP films with in-plane uniaxial alignment. The alignment of mesogens is disturbed by *tran–cis* photoisomerization of azobenzene moieties, which leads to contraction of the film surface. Under this experimental condition with relatively low intensity of UV light, the contribution of the photothermal effect is regarded to be small, as the shape recovery was slight in the dark upon turning off the UV light.[58] Fig. 2b and Movie S1 (ESI†) show photoinduced bending behaviour of a curved film with an inflection programmed at 120 °C. Upon irradiation with UV light from the top, areas with U-shape (concave upward) showed an increase in curvature, whereas those with inverted U-shape (concave downward) displayed a decrease in curvature. Although the mechanism of the deformation is essentially the same as that of a flat film, complexity in deformation is enhanced.

PAzo/PMMA IPN films with homeotropic alignment were also prepared. In this case, irradiation of a flat film with UV light leads to bending away from the light source due to the expansion of the irradiated surface (Fig. 2c).[59] The curved films programmed at 120 °C also showed reversible deformation (Fig. 2d, Movie S2, ESI†). In the current IPN system, the initial alignment of mesogens and the temporary shape of the sample can be separately controlled: the former is determined during

Published on 09 1401. Downloaded on 25/02/1405 11:07:51 ..

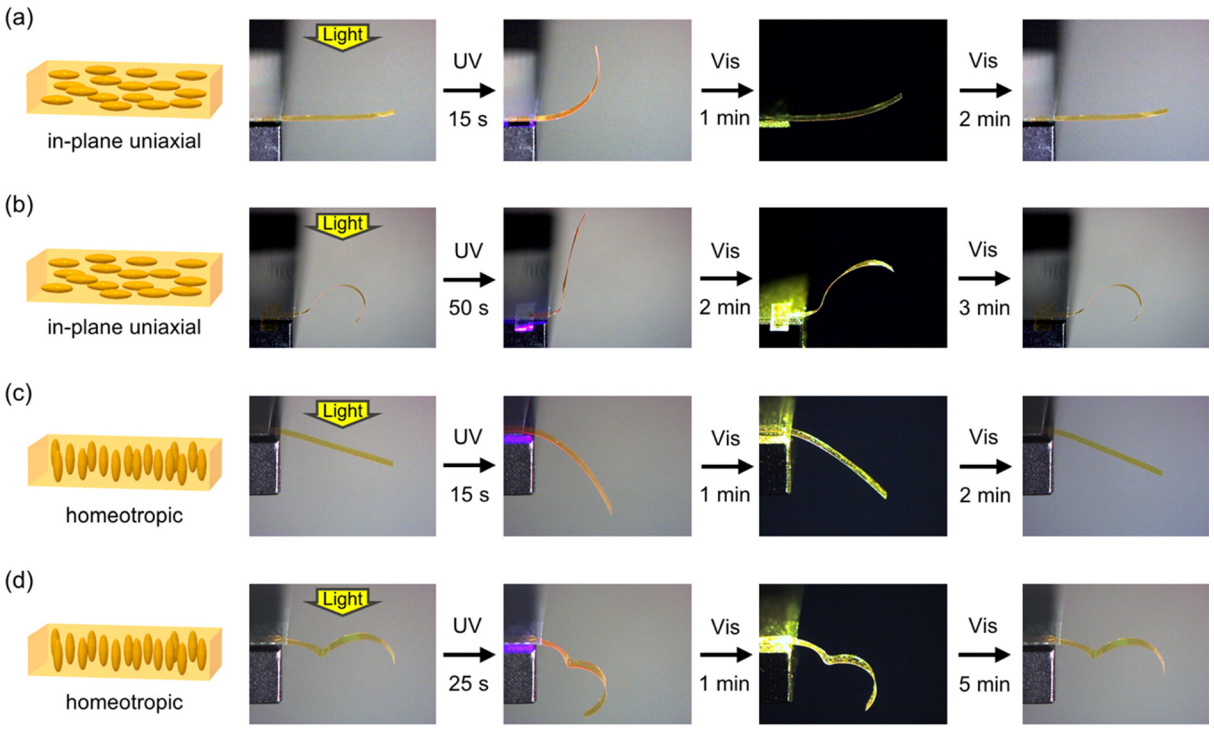

Fig. 2 Photoinduced deformation behaviours of PAzo/PMMA IPN films upon irradiation with UV (365 nm, 10 mW cm^{-2}) and visible light (>540 nm, 30 mW cm^{-2}). (a) A flat film with in-plane uniaxial alignment. Film size: 12 mm × 1 mm × 10 μm. (b) A curved film with in-plane uniaxial alignment after shape programming at 120 °C. (c) A flat film with homeotropic alignment. Film size: 12 mm × 1 mm × 6 μm. (d) A curved film with homeotropic alignment after shape programming at 120 °C.

polymerization, and the latter is fixed under heating after the formation of the network structure.

To further demonstrate the various 3D motions in IPN systems, we prepared samples with spiral shapes from PAzo/PMMA IPN films with in-plane uniaxial and homeotropic alignments. As shown in Fig. 3 and Movies S3 and S4 (ESI†), the spiral with in-plane uniaxial alignment showed unwinding motion upon irradiation with UV light, whereas the spiral with homeotropic alignment showed winding motion. These motions are attributed to contraction and expansion of the outer side of the spirals with in-plane uniaxial and homeotropic spirals, respectively. Upon irradiation with UV light, both films reverted to the original spiral shapes. The alignment control with surface layers is one of the most essential advantages in crosslinked LCPs prepared by *in situ* polymerization methods in cells. Incorporation of additional components into crosslinked LCPs allows both molecular alignment and initial shapes to be controlled separately, which would contribute to increase the variety of photoinduced deformation of photomobile materials.

The superior thermal stability of temporary shapes in IPN systems implies photodeformability at high temperatures. We investigated the photoinduced deformation of a wavy-shaped sample, which was programmed under heating at 170 °C from a flat film (thickness: 20 μm) with in-plane uniaxial alignment (Fig. 4, Movie S5, ESI†). At room temperature, the deformation was small due to the relatively large thickness of 20 μm, which

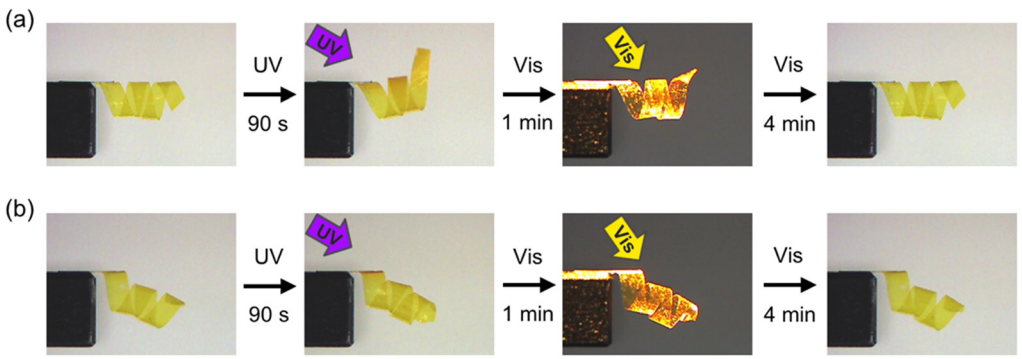

Fig. 3 Photoinduced deformation behaviors of PAzo/PMMA IPN samples with spiral shapes upon irradiation with UV (365 nm, 20 mW cm^{-2}) and visible light (>540 nm, 40 mW cm^{-2}). (a) In-plane uniaxial alignment. (b) Homeotropic alignment. Original sizes of the films: 20 mm × 1 mm × 8 μm.

 This journal is © The Royal Society of Chemistry 2023

Published on 09 1401. Downloaded on 25/02/1405 11:07:51 ..

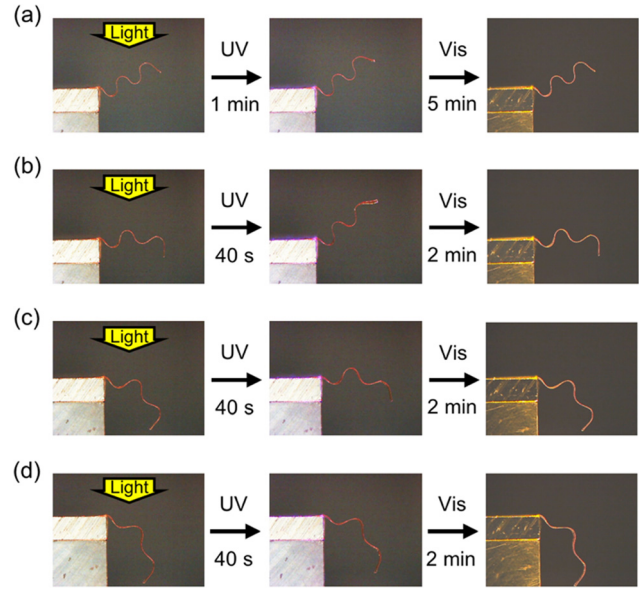

Fig. 4 Photoinduced deformation behaviours of a PAzo/PMMA IPN film with a wavy shape at (a) room temperature, (b) 100 °C, (c) 120 °C and (d) 140 °C. UV: 15 mW cm^{-2}. Vis: 10 mW cm^{-2}. The original size of the film: 20 mm × 1 mm × 19 μm.

increases flexural rigidity. At 100 °C, on the other hand, the sample showed large deformation upon irradiation with UV light. This enhancement of photoinduced bending is consistent with the decrease in elastic modulus at elevated temperatures (Fig. 1b). On the other hand, the photoinduced deformation became smaller with the increase in temperature above 100 °C. This suppression of the deformation above 100 °C is ascribed to the increase in the rate of *cis–trans* back thermal isomerization. In order to further elucidate the temperature dependence, we recorded the real-time absorption spectra of an IPN film (thickness: 3 μm) upon irradiation with UV light at various temperatures (Fig. S3, ESI†). The photoinduced changes in absorption spectra were large at room temperature and at 100 °C, which became small at 120 and 140 °C due to the fast *cis–trans* back thermal isomerization. Thus, the temperature dependence of the photoinduced bending behaviour is dominated by the balance between the elastic modulus and the rate of *cis–trans* thermal isomerization. It is noteworthy that the initial wavy shape of the sample in Fig. 4 was almost retained under heating at 100 °C. The thermal stability of non-flat temporary shapes allows various 3D motions under high-temperature conditions.

Conclusions

We investigated the shape memory effects of PAzo/PMMA IPN films in comparison with pristine PAzo films. IPN films showed gradual glass transition over a wide temperature range, which enabled shape programming at elevated temperatures. Various 3D deformations were observed for IPN samples depending on programmed temporary shapes upon irradiation with UV and visible light. IPN films with homeotropic alignment also showed reversible photoinduced deformation from 3D temporary shapes. The samples programmed at 170 °C exhibited superior thermal stability, allowing photoinduced deformation at 100 °C.

As the surface alignment methods allow precise patterning through the photoalignment technique, multiple control of the alignment of mesogens and macroscopic shapes can be a powerful approach to greatly increase the variety of photoinduced deformation. Also, the sequential formation of IPN would be applicable to various combinations of polymers, enabling control of mechanical and photoresponsive properties including deformation modes. The flexible design of photomobile materials would lead to polymer photoactuators with required functions and performance.

Author contributions

T. U. and T. I. designed the study. T. U. and K. N. carried out the experiments and analysed the results. T. I. supervised the project. T. U. wrote the manuscript in consultation with K. N. and T. I.

Conflicts of interest

There are no conflicts to declare.

Acknowledgements

This work was supported by JSPS KAKENHI (Grant Numbers JP18K14286, JP19K22220, JP21K05171), and Takahashi Industrial and Economic Research Foundation.

Notes and references

1 M. Warner and E. M. Terentjev, *Liquid Crystal Elastomers*, Oxford University Press, Oxford, UK, 2003.
2 C. Ohm, M. Brehmer and R. Zentel, *Adv. Mater.*, 2010, **22**, 3366–3387.
3 T. J. White and D. J. Broer, *Nat. Mater.*, 2015, **14**, 1087–1098.
4 Y. Yu, M. Nakano and T. Ikeda, *Nature*, 2003, **425**, 145.
5 T. Ikeda, J. Mamiya and Y. Yu, *Angew. Chem., Int. Ed.*, 2007, **46**, 506–528.
6 T. Ube and T. Ikeda, *Angew. Chem., Int. Ed.*, 2014, **53**, 10290–10299.
7 T. Ube and T. Ikeda, *Adv. Opt. Mater.*, 2019, **7**, 1900380.
8 F. Ge and Y. Zhao, *Adv. Funct. Mater.*, 2020, **30**, 1901890.
9 J. Küpfer and H. Finkelmann, *Makromol. Chem., Rapid Commun.*, 1991, **12**, 717–726.
10 D. J. Broer, H. Finkelmann and K. Kondo, *Makromol. Chem.*, 1988, **189**, 185–194.
11 M. Yamada, M. Kondo, J. Mamiya, Y. Yu, M. Kinoshita, C. J. Barrett and T. Ikeda, *Angew. Chem., Int. Ed.*, 2008, **47**, 4986–4988.
12 M. Camacho-Lopez, H. Finkelmann, P. Palffy-Muhoray and M. Shelley, *Nat. Mater.*, 2004, **3**, 307–310.

Published on 09 1401. Downloaded on 25/02/1405 11:07:51 ..

13 M. Yamada, M. Kondo, R. Miyasato, Y. Naka, J. Mamiya, M. Kinoshita, A. Shishido, Y. Yu, C. J. Barrett and T. Ikeda, *J. Mater. Chem.*, 2009, **19**, 60–62.
14 S. Palagi, A. G. Mark, S. Y. Reigh, K. Melde, T. Qiu, H. Zeng, C. Parmeggiani, D. Martella, A. Sanchez-Castillo, N. Kapernaum, F. Giesselmann, D. S. Wiersma, E. Lauga and P. Fischer, *Nat. Mater.*, 2016, **15**, 647–653.
15 T. J. White, N. V. Tabiryan, S. V. Serak, U. A. Hrozhyk, V. P. Tondiglia, H. Koerner, R. A. Vaia and T. J. Bunning, *Soft Matter*, 2008, **4**, 1796–1798.
16 A. H. Gelebart, D. J. Mulder, M. Varga, A. Konya, G. Vantomme, E. W. Meijer, R. L. B. Selinger and D. J. Broer, *Nature*, 2017, **546**, 632–636.
17 H. Zeng, M. Lahikainen, L. Liu, Z. Ahmed, O. M. Wani, M. Wang, H. Yang and A. Priimagi, *Nat. Commun.*, 2019, **10**, 5057.
18 J. Lv, Y. Liu, J. Wei, E. Chen, L. Qin and Y. Yu, *Nature*, 2016, **537**, 179–184.
19 L. T. de Haan, C. Sánchez-Somolinos, C. M. W. Bastiaansen, A. P. H. J. Schenning and D. J. Broer, *Angew. Chem., Int. Ed.*, 2012, **51**, 12469–12472.
20 T. H. Ware, M. E. McConney, J. J. Wie, V. P. Tondiglia and T. J. White, *Science*, 2015, **347**, 982–984.
21 L. T. de Haan, V. Gimenez-Pinto, A. Konya, T.-S. Nguyen, J. M. N. Verjans, C. Sánchez-Somolinos, J. V. Selinger, R. L. B. Selinger, D. J. Broer and A. P. H. J. Schenning, *Adv. Funct. Mater.*, 2014, **24**, 1251–1258.
22 O. M. Wani, H. Zeng, P. Wasylczyk and A. Priimagi, *Adv. Opt. Mater.*, 2018, **6**, 1700949.
23 Y. Sawa, F. Ye, K. Urayama, T. Takigawa, V. Gimenez-Pinto, R. L. B. Selinger and J. V. Selinger, *Proc. Natl. Acad. Sci. U. S. A.*, 2011, **108**, 6364–6368.
24 S. Iamsaard, S. J. Aßhoff, B. Matt, T. Kudernac, J. J. L. M. Cornelissen, S. P. Fletcher and N. Katsonis, *Nat. Chem.*, 2014, **6**, 229–235.
25 C. P. Ambulo, J. J. Burroughs, J. M. Boothby, H. Kim, M. R. Shankar and T. H. Ware, *ACS Appl. Mater. Interfaces*, 2017, **9**, 37332–37339.
26 M. del Pozo, J. A. H. P. Sol, A. P. H. J. Schenning and M. G. Debije, *Adv. Mater.*, 2022, **34**, 2104390.
27 Z. Wang and S. Cai, *J. Mater. Chem. B*, 2020, **8**, 6610–6623.
28 T. Ube, K. Kawasaki and T. Ikeda, *Adv. Mater.*, 2016, **28**, 8212–8217.
29 Y. Li, O. Rios, J. K. Keum, J. Chen and M. R. Kessler, *ACS Appl. Mater. Interfaces*, 2016, **8**, 15750–15757.
30 Z.-C. Jiang, Y.-Y. Xiao, X. Tong and Y. Zhao, *Angew. Chem., Int. Ed.*, 2019, **58**, 5332–5337.
31 Y. Wu, Y. Yang, X. Qian, Q. Chen, Y. Wei and Y. Ji, *Angew. Chem., Int. Ed.*, 2020, **59**, 4778–4784.
32 Z.-C. Jiang, Y.-Y. Xiao, L. Yin, L. Han and Y. Zhao, *Angew. Chem., Int. Ed.*, 2020, **59**, 4925–4931.
33 T. S. Hebner, M. Podgorski, S. Mavila, T. J. White and C. N. Bowman, *Angew. Chem., Int. Ed.*, 2022, **61**, e202116522.
34 M. Lahikainen, H. Zeng and A. Priimagi, *Nat. Commun.*, 2018, **9**, 4148.
35 A. H. Gelebart, D. J. Mulder, G. Vantomme, A. P. H. J. Schenning and D. J. Broer, *Angew. Chem., Int. Ed.*, 2017, **56**, 13436–13439.
36 A. Lendlein and R. Langer, *Science*, 2002, **296**, 1673–1676.
37 A. Lendlein, H. Jiang, O. Jünger and R. Langer, *Nature*, 2005, **434**, 879–882.
38 X. Zhang, C. Zhu, B. Xu, L. Qin, J. Wei and Y. Yu, *ACS Appl. Mater. Interfaces*, 2019, **11**, 46212–46218.
39 R. C. P. Verpaalen, M. P. daCunha, T. A. P. Engels, M. G. Debije and A. P. H. J. Schenning, *Angew. Chem., Int. Ed.*, 2020, **59**, 4532–4536.
40 T. Ube, K. Takado and T. Ikeda, *J. Mater. Chem. C*, 2015, **3**, 8006–8009.
41 T. Ube, K. Minagawa and T. Ikeda, *Soft Matter*, 2017, **13**, 5820–5823.
42 J. E. Stumpel, E. R. Gil, A. B. Spoelstra, C. W. M. Bastiaansen, D. J. Broer and A. P. H. J. Schenning, *Adv. Funct. Mater.*, 2015, **25**, 3314–3320.
43 H.-F. Lu, M. Wang, X.-M. Chen, B.-P. Lin and H. Yang, *J. Am. Chem. Soc.*, 2019, **141**, 14364–14369.
44 X. Lin, W. Zou and E. M. Terentjev, *Macromolecules*, 2022, **55**, 810–820.
45 M. Moirangthem, T. A. P. Engels, J. Murphy, C. W. M. Bastiaansen and A. P. H. J. Schenning, *ACS Appl. Mater. Interfaces*, 2017, **9**, 32161–32167.
46 D. C. Hoekstra, M. G. Debije and A. P. H. J. Schenning, *Macromolecules*, 2021, **54**, 5410–5416.
47 G. Q. Liu, X. B. Ding, Y. P. Cao, Z. H. Zheng and Y. X. Peng, *Macromol. Rapid Commun.*, 2005, **26**, 649–652.
48 D. Ratna and J. Karger-Kocsis, *Polymer*, 2011, **52**, 1063–1070.
49 Y. Wu, J. L. Hu, J. Han, Y. Zhu, H. Huang, J. Li and B. Tang, *J. Mater. Chem. A*, 2014, **2**, 18816–18822.
50 C. Wang, Y. Zhang, J. Li, Z. Yang, Q. Wang, T. Wang, S. Li, S. Chen and X. Zhang, *Eur. Polym. J.*, 2020, **123**, 109393.
51 A. S. Angeloni, D. Caretti, C. Carlini, E. Chiellini, G. Galli, A. Altomare, R. Solaro and M. Laus, *Liq. Cryst.*, 1989, **4**, 513–527.
52 D. J. Broer, J. Boven, G. N. Mol and G. Challa, *Makromol. Chem.*, 1989, **190**, 2255–2268.
53 J. L. G. Ribelles, M. M. Pradas, J. M. M. Duenas and C. T. Cabanilles, *J. Non-Cryst. Solids*, 2002, **307**, 731–737.
54 L. H. Sperling, in *Interpenetrating Polymer Networks*, ed. D. Klempner, L. H. Sperling and L. A. Utracki, American Chemical Society, Washington, D.C., 1994, Ch. 1, pp. 3–38.
55 Y. Zhao and G. X. Yuan, *Macromolecules*, 1996, **29**, 1067–1069.
56 P. Miaudet, A. Derre, M. Maugey, C. Zakri, P. M. Piccione, R. Inoubli and P. Poulin, *Science*, 2007, **318**, 1294–1296.
57 T. Xie, *Nature*, 2010, **464**, 267–270.
58 M. P. da Cunha, E. A. J. van Thoor, M. G. Debije, D. J. Broer and A. P. H. J. Schenning, *J. Mater. Chem. C*, 2019, **7**, 13502–13509.
59 M. Kondo, Y. Yu and T. Ikeda, *Angew. Chem., Int. Ed.*, 2006, **45**, 1378–1382.

 This journal is © The Royal Society of Chemistry 2023